

# ReMP: Reusable Motion Prior for Multi-domain 3D Human Pose Estimation and Motion Inbetweening

Hojun Jang<sup>1</sup> and Young Min Kim<sup>1,2</sup>

<sup>1</sup> Dept. of Electrical and Computer Engineering, Seoul National University

<sup>2</sup> Interdisciplinary Program in Artificial Intelligence and INMC, Seoul National University

{j12040208, youngmin.kim}@snu.ac.kr

## Abstract

We present *Reusable Motion prior (ReMP)*, an effective motion prior that can accurately track the temporal evolution of motion in various downstream tasks. Inspired by the success of foundation models, we argue that a robust spatio-temporal motion prior can encapsulate underlying 3D dynamics applicable to various sensor modalities. We learn the rich motion prior from a sequence of complete parametric models of posed human body shape. Our prior can easily estimate poses in missing frames or noisy measurements despite significant occlusion by employing a temporal attention mechanism. More interestingly, our prior can guide the system with incomplete and challenging input measurements to quickly extract critical information to estimate the sequence of poses, significantly improving the training efficiency for mesh sequence recovery. ReMP consistently outperforms the baseline method on diverse and practical 3D motion data, including depth point clouds, LiDAR scans, and IMU sensor data. Project page is available in <https://hojunjang17.github.io/ReMP>.

## 1. Introduction

Foundation models have recently demonstrated the power of large-scale datasets, demonstrating innovative results in diverse downstream tasks. However, compared to natural language processing [2, 6, 28] (trained with 350 GB-45 TB of data), or image processing [4, 19, 31] (trained with 10-400 million images), the counterpart of human motion has remained less explored. Although we may not be able to collect an internet scale of data with accurate human motion, we argue that existing motion data, such as AMASS [26] (~ 11,000 motions), are sufficient to learn a strong motion prior. Compared to the possible space of image pixels or arrangement of words, the space of possible human body poses is relatively more constrained and can be

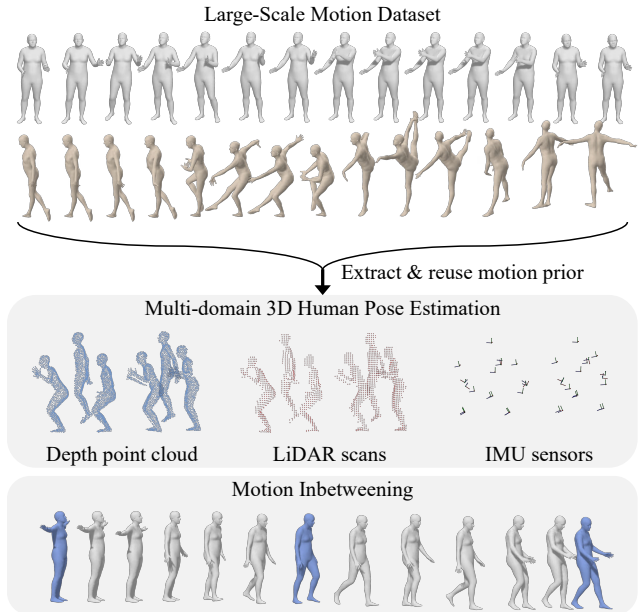


Figure 1. We extract rich motion priors from the large-scale motion dataset and reuse them for various applications, such as 3D human pose estimation and motion inbetweening.

successfully modeled with a handful set of parameters [23]. If we consider the temporal sequence of motion, only a subset of pose sequences is physically plausible and realistic, confined by the human body’s skeletal structure and natural capabilities.

Our prior deliberately focuses on accurately reconstructing human mesh sequences with 3D dynamic information. The prior knowledge can be adapted to other modalities and various downstream tasks that require the capture of 3D motion. In contrast to the abundant literature that estimates poses in 2D images or video inputs [9, 13, 25, 33, 42], our prior is composed of complete 3D configurations that are free from projective distortion, occlusion, or appearance changes. We also examine a temporal sequence of mo-

tion instead of estimating frame-wise poses, which should incorporate temporal context, increasing the robustness of estimation in various adversaries. The 3D action space with temporal context can better represent human intents and gestures or temporally predict subsequent motions, enabling us to develop applications that accurately capture human motion or provide necessary services.

In this paper, we obtain a Reusable Motion Prior (ReMP), which contains a tight correlation in 3D temporal sequences from existing datasets [26]. We take a sequence of motion and use a temporal transformer followed by a variational autoencoder (VAE) architecture to obtain a latent distribution. The comprehensive parameters provide the geometric variations within the movement, while the transformer applies attention to temporal dependencies. Our training formulation is specifically designed to capture fine-grained motion variations within the sequence of motion. Specifically, we adapt continuous latent representation to maximize expressivity and maintain a temporal sequence of latent embeddings that correspond to individual time stamps for the encoded sequence. We apply random masking in the transformer during training to promote modeling temporal context. We also incorporate effective input encodings, such as 6D rotation representation, incremental translation, and velocities, and allow the neural network to comprehend detailed dynamics. Compared to generative priors, our latent space can accurately track the full 3D mesh of human poses.

Once we obtain a comprehensive prior from complete 3D data, we can reuse the prior to extract essential information from various measurement characteristics. We propose a distillation method that adapts the prior to estimate plausible 3D motion even under noisy, incomplete data or fill the in-between motions given sparse poses. Even when the data is occluded or sparse, our motion prior encourages the network to detect critical features and quickly train the network to perform motion estimation. Our work can also regress motion parameters in other modalities that measure dynamic human movements, such as IMU, and show robust performance to estimate accurate movement. The aid of pretrained motion prior additionally enhances efficiency and results in better performance than the baselines in smaller training datasets.

In summary, our contributions are threefold:

- We introduce ReMP, a novel framework for learning reusable motion prior from large-scale 3D motion dataset, which significantly enhances accuracy and robustness in human pose estimation and motion inbetweening tasks.
- We demonstrate an effective formulation for 3D motion prior that can accurately encode dynamic dependencies inherent in human motion sequences that can

increase the data usage efficiency.

- We present remapping techniques of our pretrained motion prior to different measurements or various adversaries, demonstrating its versatility and efficiency across diverse motion capture modalities.

## 2. Related Works

### 2.1. Motion Prior

Similar to the success of foundation models, many works in human motion understanding leverage large-scale datasets to enhance performance in various tasks. While there exists rich literature that finds a latent space for individual poses, we specifically focus on works that incorporate temporal correlations between adjacent frames within a motion sequence. Motion VAE [21] and HuMoR [32] are notable examples, which employ a conditional variational autoencoder (CVAE) architecture to learn generative priors of the future frame conditioned on the current frame. MotionVAE leverages the prior to generate goal-directed human motion within a reinforcement-learning framework, while HuMoR initializes poses from the prior and further refines them through heavy optimization steps.

Other works capture rich dynamic information from a temporal span of motion sequences longer than two consecutive frames. To avoid posterior collapse that is prevalent with generative priors, additional information often provides structural guidance in the latent space. Actor [29] learns a prior combined with action labels, such that a latent code can be generated conditioned on action labels or text descriptions. PoseGPT [24] and MoMask [11] map motion sequences to a discrete latent space using a vector-quantized variational autoencoder (VQVAE) [36] architecture, which can produce a sequence of motions by estimating an index of the codebook.

In contrast, our proposed method learns more expressive continuous latent space and mainly focuses on correctly reconstructing 3D full-body motion. Our priors are exclusively trained from motion sequences without relying on action labels or text descriptions. Jang *et al.* [15] demonstrated that spatio-temporal prior can effectively recover full-body mesh sequences from point cloud input. Our work learns a more general prior extracted from a parametric model. The motion prior from ReMP is more comprehensive and flexible, allowing it to understand 3D human motion from diverse input modalities.

### 2.2. 3D Human Pose Estimation

Estimating an accurate human motion from diverse sensor data has gained significant attention due to a wide range of possible applications, such as lightweight motion capture, human-machine interaction, and human behavior analysis. Our proposed prior includes the temporal context of

3D motion and can enhance the accuracy of pose estimations in various contexts with diverse sensor modalities. Previous works rely on tracking devices with carefully calibrated cameras, or individual frames are processed separately. Even when using more casual input modalities, most previous works require separate training of the model for different tasks or input modalities.

**Depth Camera** A depth camera is one of the most practical inputs to estimate 3D human motion. While the data may suffer from occlusions and measurement noises, commodity devices can quickly obtain 3D measurements of humans without further calibration or markers. A large volume of previous works processes individual frames to obtain a reasonable estimate, which leads to unnatural jittering in estimated poses [10, 22, 45]. Jang *et al.* [15] increases the time span to longer motion sequences and directly estimates the motions without optimization in point cloud input. ReMP further demonstrates incorporating a coherent motion prior to different input modalities.

**LiDAR** LiDAR is one of the most widely used 3D sensors, especially for autonomous driving, and there is a demand for accurate human motion recognition in the data. While depth cameras and LiDAR both capture point cloud measurements, LiDAR measurements are significantly sparser than depth camera outputs, making human pose estimation from LiDAR data more challenging. Furthermore, few LiDAR datasets are available to train reliable human pose estimation models. Some LiDAR scan datasets contain human motion [3, 34] but lack accurate ground truth pose annotations. Some works provide LiDAR scan to SMPL annotations [5, 7, 20], but they contain limited data and may lack the quality needed to train accurate pose estimation models. By leveraging reusable motion prior and our synthetically generated dataset, we can estimate accurate temporal motion in challenging LiDAR datasets, overcoming the limitations of sparse data and the lack of comprehensive ground truth annotations.

**IMU Sensor** IMU sensors, commonly used in AR/VR and wearable devices, are cost-effective devices that can be directly attached to body parts to reconstruct human motion. SIP [39] was among the first to utilize IMU sensor data for human pose estimation, optimizing pose parameters to match the input sensor data. Subsequent works, such as DIP-IMU [14], employed deep learning architectures like RNNs for pose estimation. Recent advancements, including [16, 40, 41], have enhanced performance by integrating physics-based constraints. ReMP leverages a pretrained motion prior from a large-scale motion dataset, which leads to physically plausible motion sequences that adhere to the physical constraints of the human body.

### 3. Method

We encode the full 3D mesh of diverse human poses with SMPL [23]. SMPL is the most widely used parametric human model to map the full-body mesh composed of 6890 vertices  $V \in \mathbb{R}^{6890 \times 3}$  into a set of parameters. The parameters include pose parameters  $\theta \in \mathbb{R}^{24 \times 3}$ , root translation  $x \in \mathbb{R}^3$ , and shape parameters  $\beta \in \mathbb{R}^{10}$ . We convert the pose parameter from an axis-angle representation to a 6D rotation representation  $\theta_{6D} \in \mathbb{R}^{24 \times 6}$ , which is more suitable for training neural networks and resolves the ambiguity issue [12]. Following [32], we use the difference in root translation between consecutive frames ( $\Delta x$ ) in the global coordinate system rather than the absolute value. Naïve concatenation of translation to pose parameters often overlooks discrepancies due to dimensional imbalance. To address this, we expand the dimensionality of  $\Delta x$  using a simple MLP to match the dimensions of  $\theta_{6D}$ , and then concatenate them to form the motion parameters for a single pose

$$M = \left[ \theta_{6D}^{\text{flat}}, \text{MLP}_{3 \rightarrow 144}(\Delta x) \right] \in \mathbb{R}^{144+144}. \quad (1)$$

Then, we represent human motion using a sequence of motion parameters  $M_{1:T}$ . We validate the use of  $\Delta x$  instead of the absolute translation value and the dimension expansion to  $\Delta x$  in the supplementary material.

Our method consists of two main steps as described in Figure 2. In the first phase, we train motion prior and learn the temporal context of the motion parameter sequence (Sec. 3.1). The second reusing phase learns to perform various tasks using the trained motion prior (Sec. 3.2).

#### 3.1. Training Motion Prior

We train the motion prior with a large-scale motion dataset containing diverse motions. At a high level, our approach follows the regular variational autoencoder (VAE) [18] training scheme. We employ a continuous latent space to express fine-grained motion accurately. We use a VAE architecture based on a transformer network [38] as the backbone. The transformer encoder takes the motion parameters  $M_{1:T} \in \mathbb{R}^{T \times 288}$  as input to create a motion feature  $z'_{1:T} \in \mathbb{R}^{T \times D_z}$ . Each transformer input channel takes a single motion parameter, with positional embeddings added, to effectively learn the temporal correlations of the motion. The motion sequence of length  $T$  is embedded into a sequence of continuous latent variables of the same length, allowing a sufficiently rich latent space to capture fine-grained motion variations. Using the motion feature vector, we employ separate 2-layer MLPs to generate a posterior distribution  $q_\phi(z_t | M_t, z'_t)$  and a prior distribution  $p_\psi(z_t | z'_t)$ , where  $z_t \in \mathbb{R}^{D_z}$  is a latent vector at the  $t^{\text{th}}$  time step. We assume Gaussian distributions for both the posterior and prior distributions. After sampling  $z_{1:T}$

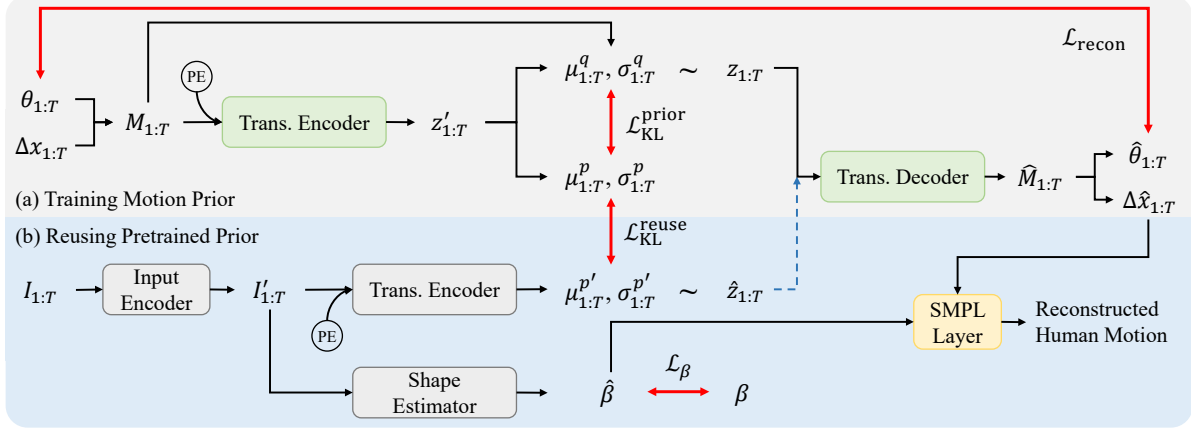


Figure 2. The overall pipeline of our method consists of two parts: (a) training motion prior and (b) reusing pretrained prior. In the motion prior training phase, a sequence of pose parameters  $\theta_{1:T}$  and the root translation transitions  $\Delta x_{1:T}$  form a sequence of motion parameter  $M_{1:T}$ . We use a transformer encoder and MLP layers to generate Gaussian distributions where we can sample the latent vectors. We feed the latent vectors to a transformer decoder to generate the motion parameters then to the SMPL parameters. After training the prior, we freeze all the networks used in the first phase. In the reusing phase, we encode the input data and use a transformer encoder to generate a distribution that is then used to sample the latent vectors for the transformer decoder. We use an additional shape parameter estimator for  $\beta$ . Finally, we combine all three parameters with the SMPL layer to reconstruct the human motion.

from these distributions, we input the latent vectors into the transformer decoder to reconstruct the SMPL parameters.

Our reconstruction loss covers comprehensive aspects of motion reconstruction. Specifically, we use the following loss terms to train the posterior distribution:

$$\mathcal{L}_{\text{recon}} = \sum_{s \in S} w_s \mathcal{L}_s, \quad S = \{\theta, \Delta\theta, x, \Delta x, J, V\} \quad (2)$$

$\mathcal{L}_{\theta}$  is a pose parameter difference loss, which is L2 distance between the estimated and the ground truth 6D pose parameters.  $\mathcal{L}_{\Delta\theta}$  is an angular velocity loss, which makes the angular velocity of the estimated pose parameter match the ground truth.  $\mathcal{L}_x$  and  $\mathcal{L}_{\Delta x}$  are the loss terms that make the estimated root translation position and its speed to be similar to the ground truth, respectively. Finally,  $\mathcal{L}_J$  and  $\mathcal{L}_V$  are the L2 distance between the estimated joints and vertices to be near the ground truth, respectively. Additionally, we encourage the prior distribution to follow the posterior distribution using a KL divergence loss:

$$\mathcal{L}_{\text{KL}}^{\text{prior}} = \frac{1}{T} \sum_t D_{KL}(q_{\phi}(z_t | M_t, z'_t) \| p_{\psi}(z_t | z'_t)). \quad (3)$$

The total loss function to train motion prior is as follows:

$$\mathcal{L}_{\text{prior}} = \mathcal{L}_{\text{recon}} + w_{\text{KL}}^{\text{prior}} \mathcal{L}_{\text{KL}}^{\text{prior}}. \quad (4)$$

For better generalizability, we randomly mask some frames of the input motion parameters by utilizing a `key_padding_mask` in the transformer encoder. The random temporal mask helps our model to better encode the

unseen motion sequence and increase robustness to our motion autoencoder. Thanks to the use of input masking, our model can also perform motion inbetweening task.

### 3.2. Reusing Pretrained Prior

After training the motion prior with the large-scale dataset, we freeze the networks and reuse the rich motion prior to reconstructing motions for different input conditions. Our reusing phase mainly consists of two parts: an input encoder that processes different inputs, followed by a latent mapper, which brings the encoded input into the pretrained latent space from the first phase. These transforms can be quickly trained with relatively a small amount of data, even with synthetic data, and such that we can effectively exploit the motion context of reusable prior, which is further demonstrated in Sec. 4.

As the observation from a different sensor modality comes in, the input encoder encodes the data  $I_{1:T}$  to a meaningful feature  $I'_{1:T} \in \mathbb{R}^{T \times D'_I}$ . We use PointNet [30] as the input encoder for the point cloud input and 2-layer MLP for the IMU data input. The encoded features are then put into the latent mapper, which is also a transformer encoder. The latent mapper generates the Gaussian distribution  $p'_{\psi}(z_t | I'_t)$  that can be used to sample the latent vectors from the input features. The distribution is forced to follow the distribution of the prior distribution  $p_{\psi}$  by a KL divergence loss

$$\mathcal{L}_{\text{KL}}^{\text{reuse}} = \frac{1}{T} \sum_t D_{KL}(p_{\psi}(z_t | z'_t) \| p'_{\psi}(z_t | I'_t)). \quad (5)$$

Also, for better estimation performance, we leverage the

same loss terms used to train the posterior distribution  $q_\phi$  as shown in Eq. (2).

As motion prior does not contain information about the shape parameters  $\beta$ , we have an additional shape parameter estimator. Shape parameter estimator is a 2-layer MLP that receives an encoded input feature  $I'_{1:T}$  as an input and outputs an estimate  $\hat{\beta}$ . The shape parameter should not change during the motion, so we flatten  $I'_{1:T}$  into a one-dimensional vector and put it to the shape estimator MLP to generate a single  $\hat{\beta}$  for each sequence. To train the shape estimator, we use a weighted loss function that penalizes more to the former part of  $\beta \in \mathbb{R}^{10}$  as the shape parameters are the result of PCA. That is, we use our shape loss to be

$$\mathcal{L}_\beta = \sum_{i=1}^{10} \frac{11-i}{10} (\beta_i - \hat{\beta}_i)^2. \quad (6)$$

Therefore, the final loss function to train reusing the prior is

$$\mathcal{L}_{\text{reuse}} = \mathcal{L}_{\text{recon}} + w_{\text{KL}}^{\text{reuse}} \mathcal{L}_{\text{KL}}^{\text{reuse}} + w_\beta \mathcal{L}_\beta. \quad (7)$$

## 4. Experiments

This section demonstrates how the prior motion is reused for downstream tasks. First, we present the results of ReMP, showing its superior performance over baselines in versatile 3D human pose estimation tasks in various sensor modalities (Sec. 4.1) and motion inbetweening (Sec. 4.2). We also highlight the effectiveness of motion prior in Sec. 4.3.

**Synthetic Dataset Generation** Our outputs require accurate SMPL parameters for supervision using  $\mathcal{L}_{\text{recon}}$ . However, datasets containing both input sensor data and accurate SMPL parameters are rare. We, therefore, first generate training datasets for different input modalities, following the method introduced in the previous works [14, 15, 37]. We utilize the AMASS dataset [26] for both motion prior training and the reusing phases of our method. The AMASS dataset is a comprehensive human motion dataset comprising approximately 11,000 motion sequences with SMPL parameters, providing ample data to learn rich motion priors.

For the reusing phase, we generate synthetic datasets for each input modality. Using the Open3D library [44], we render SMPL meshes and generate depth images, which are then converted into point clouds. We create dense depth images for synthetic depth point clouds and sparse depth images for LiDAR point clouds, using 1,024 and 256 points, respectively. For the IMU dataset, we attach six synthetic IMUs to the SMPL mesh and track the acceleration and orientation of each sensor during the movements. Each sequence is generated with 40 frames at a framerate of 10 fps. We show additional details of the data generation process in the supplementary material.

Method	Synthetic CMU			B-MHAD
	Pose [°]	Joint [cm]	Mesh [cm]	CD [cm]
VoteHMR [22]	6.71	13.76	15.20	28.31
Zuo <i>et al.</i> [45]	7.58	14.78	16.23	31.56
Jang <i>et al.</i> [15]	5.43	11.15	12.62	18.71
ReMP <sup>†</sup>	6.37	18.58	20.47	25.59
<b>ReMP</b>	<b>4.90</b>	<b>9.89</b>	<b>11.16</b>	<b>17.61</b>

Table 1. Comparison with the previous methods, which reconstruct SMPL parameters from depth point clouds, on synthetic (CMU [17]) and real-world (B-MHAD, Berkeley MHAD [27]) datasets. ReMP<sup>†</sup> refers to the model directly trained on synthetic AMASS [26] without using the motion prior.

After synthetic training, we can directly test our method on real-world datasets. The synthetic datasets provide accurate 3D motion information, which is robust and effective in practical scenarios.

### 4.1. Motion Estimation

We compare the performance of 3D human pose estimation against state-of-the-art methods for depth point cloud, LiDAR, and IMU inputs. The supplementary material contains descriptions on the baseline methods and additional results with videos. ReMP excels in human pose estimation in all scenarios without the need for additional information or heavy optimization steps, demonstrating robust and versatile performance across different tasks.

**Depth Point Cloud** We evaluate the 3D human pose estimation performance of ReMP and the baselines [15, 22, 45] trained on the synthetic AMASS dataset. Firstly, we test ReMP on the synthetic CMU [17] dataset, which is part of the larger synthetic AMASS dataset we generated. This dataset was not seen during training. Secondly, we evaluate ReMP on Berkeley MHAD dataset [27], captured using a Microsoft Kinect sensor [43], to demonstrate the applicability of ReMP on real-world data. Given that the Berkeley MHAD dataset is an unsegmented depth image including surrounding environments, we preprocess it by roughly cropping the points near the actor using a bounding box.

We use four time-averaged metrics to evaluate the performance. Pose error is the angular difference between the ground truth and the estimated pose parameters. Joint and mesh errors are the Euclidean distance errors of the joints and mesh vertices, respectively. Finally, Chamfer distance [8] is used to evaluate the Berkeley MHAD dataset since it does not contain ground truth SMPL parameters.

Table 1 presents the quantitative results of our method compared to baselines on both the synthetic and real datasets. ReMP consistently outperforms all baselines across every metric, demonstrating its robustness and effective



Figure 3. Results of ReMP and the baselines on synthetic CMU [17] depth point cloud data. The colors on the mesh indicate the displacement from the ground truth vertices.

Method	SLOPER4D		
	Pose [°]	Joint [cm]	Mesh [cm]
VoteHMR [22]	8.59	36.33	53.79
Zuo <i>et al.</i> [45]	10.48	43.85	43.87
Jang <i>et al.</i> [15]	<b>8.57</b>	22.28	22.54
ReMP <sup>†</sup>	9.96	87.46	96.94
<b>ReMP</b>	8.58	<b>21.66</b>	<b>22.03</b>

Table 2. Comparison with the previous methods, which reconstruct SMPL parameters from LiDAR scan, on SLOPER4D [5] dataset. ReMP<sup>†</sup> refers to the model directly trained on synthetic AMASS [26] without using the motion prior.

tiveness. Berkeley MHAD dataset highlights ReMP’s sim-to-real performance, effectively handling real-world noise without further fine-tuning. While Jang *et al.* [15] also use a motion prior trained with point cloud, the general and comprehensive prior of ReMP results in superior performance.

Figure 3 shows the qualitative results of each method. VoteHMR [22] and Zuo *et al.* [45] struggle to reconstruct continuous motion as they find independent poses for individual frames. Jang *et al.*, in contrast, successfully estimates coherent motion throughout the sequence. However, among all methods, ReMP demonstrates the highest quality in estimated human motion.

Method	TotalCapture				
	SIP [°]	Ang [°]	Pos [cm]	Mesh [cm]	Jitter [km/s <sup>3</sup> ]
DIP [14]	18.93	17.50	9.57	11.40	35.94
TransPose [41]	16.69	12.93	6.61	7.49	9.44
PIP [40]	12.93	<b>12.04</b>	5.61	6.51	0.20
ReMP <sup>†</sup>	15.11	13.35	6.43	7.51	0.08
<b>ReMP</b>	<b>12.43</b>	12.07	<b>5.49</b>	<b>6.35</b>	<b>0.03</b>

Table 3. Comparison with the previous methods, which reconstruct SMPL parameters from IMU sensor data, on TotalCapture [35] dataset. ReMP<sup>†</sup> refers to the model directly trained on synthetic AMASS [26] without using the motion prior.

**LiDAR Scans** We test our method for the LiDAR point cloud on SLOPER4D dataset [5], which is a real LiDAR scan dataset. Table 2 shows the quantitative result of our method and the baselines on SLOPER4D, and Figure 4 visualizes the results with the error maps. The data is much more sparse and noisy compared to the depth point cloud, resulting in higher errors compared to Table 1. ReMP shows the best mesh reconstruction result among the pose estimation methods, especially for hand positions. VoteHMR [22] and Zuo *et al.* [45] fail to estimate smooth motion, as in the depth point cloud scenario.

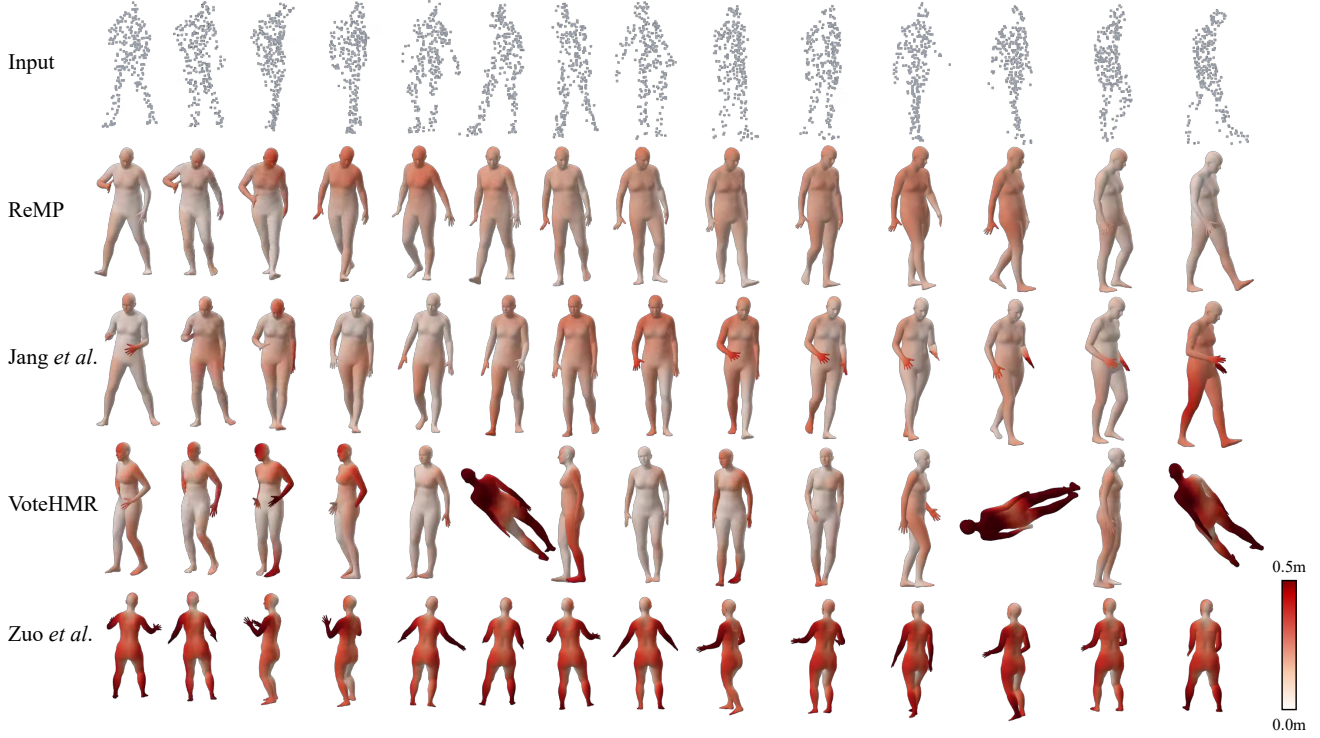


Figure 4. Pose estimation results of ReMP and the baselines on SLOPER4D dataset [5]. The colors on the mesh indicate the displacement from the ground truth vertices.

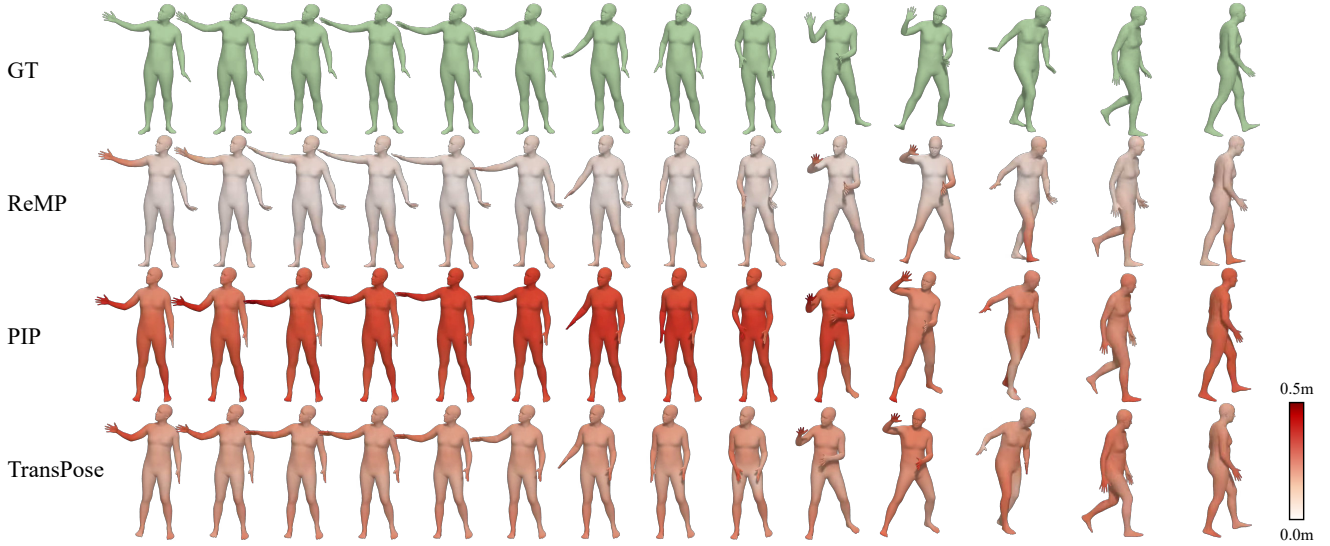


Figure 5. Motion reconstruction results of ReMP and the baselines from IMU sensor data on TotalCapture dataset [35]. The colors on the mesh indicate the displacement from the ground truth vertices.

**IMU Sensor Data** After the motion estimation module is trained with synthetic IMU datasets, we evaluate the performance on TotalCapture dataset [35], which contains real IMU measurements. We report the performance using five evaluation metrics introduced in DIP [14], which are widely used. SIP error is a mean orientation error of the upper arms and legs in the global space. Angular error is a mean global

rotation error of all body joints. Positional error and mesh error are the mean Euclidean distance errors of all estimated joints and mesh vertices, respectively, with the root joint aligned. Finally, a jitter is a mean jerk, a time derivative of the acceleration of all body joints.

We report the results of all methods in Table 3. ReMP outperforms baselines, except for the angular error which is

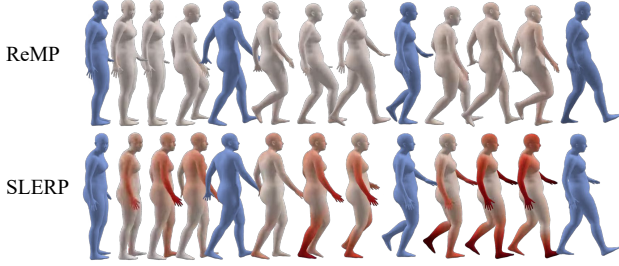


Figure 6. Motion inbetweening results of ReMP and SLERP when the blue frames are given. ReMP better generates the inbetween frames of the sequence while SLERP fails to interpolate realistic motion.

larger than PIP [40]. Jitter is the most significant enhancement over the baselines, showing that the inherent temporal coherence induces plausible motion estimation. Figure 5 emphasizes that ReMP has the best performance in recovering human motion from the IMU input. We omit the visualization of DIP since it cannot estimate root translation.

## 4.2. Motion Inbetweening

Motion inbetweening aims to interpolate between two key poses to generate intermediate frames. While linear interpolation (LERP) and spherical linear interpolation (SLERP) provide straightforward approaches, they may not always yield realistic results, particularly over longer time intervals or periodic motions such as locomotion. Leveraging motion prior, one can generate multiple plausible motion sequences starting from the initial keyframe and select the one with the closest pose of the ending keyframe pose, as proposed in Neural Marionette [1]. However, generating and comparing multiple candidates can be computationally inefficient and not guarantee precise in-betweening. ReMP, on the other hand, utilizes temporal masks while training the transformer encoder, which means we can appropriately adjust the `key_padding_mask` to learn motion in-betweening.

Figure 6 shows the result of the motion in-betweening task of ReMP and SLERP, which shows superior results compared to LERP. The error map indicates that ReMP closely recovers the original motion, while simple interpolation of SLERP fails to reconstruct detailed motion variations. We do not show the result of Neural Marionette because they use different skeletal structures and only generate output voxels instead of full parametric mesh.

## 4.3. Effects of Motion Prior

The foundational motion prior of ReMP guides various tasks of reconstructing fine-grained motions effectively. To assess the impact of motion priors, we train a variant of our model from scratch in a supervised fashion, without leveraging motion priors, referred to as ReMP<sup>†</sup>. We report the results in Tables 1, 2, and 3. In all scenarios, reusing the

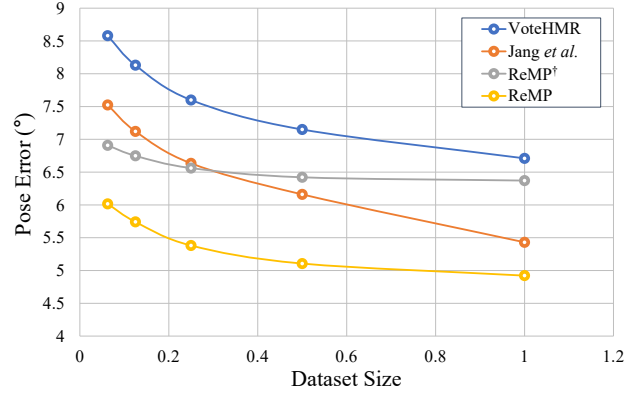


Figure 7. Error curve of ReMP and the baselines on differing dataset size.

motion prior significantly boosts the performance of human motion estimation.

To further demonstrate the effectiveness of ReMP, we conducted an experiment to evaluate its data efficiency compared to the baselines on synthetic CMU [17] dataset. We progressively reduce the training data size to 1/2, 1/4, 1/8, and 1/16 of the original dataset and observe resulting pose errors in Figure 7. ReMP achieves comparable results even when the training data is reduced to 1/4 of its original size. Moreover, ReMP maintains superior performance relative to the baselines as the dataset size decreases, underscoring its efficiency in leveraging limited training data.

## 5. Conclusion

We presented a reusable motion prior that captures rich temporal correlations of detailed 3D human motion from large-scale datasets. Leveraging this pretrained motion prior, we achieved superior performance in human pose estimation from various sensor data compared to existing methods. The module with the reusable motion prior can maintain robust performance in real sensor noises without further fine-tuning and quickly estimate accurate motions with relatively small amount of supervision, even only with synthetically generated data. Additionally, the temporal information accurately filled in the missing frames of motion sequences. We expect the versatility of ReMP can be adapted in various real-world applications requiring fast and accurate 3D human pose estimation under unknown adversaries or unstable network connections.

**Acknowledgments** This work was supported by the NRF grant (No. RS-2023-00218601) and IITP grant [No. RS-2021-II211343, Artificial Intelligence Graduate School Program (Seoul National University)] funded by the Korea government(MSIT), and Creative-Pioneering Researchers Program through Seoul National University, Young Min Kim is the corresponding author.

## References

- [1] Jinseok Bae, Hojun Jang, Cheol-Hui Min, Hyungun Choi, and Young Min Kim. Neural marionette: Unsupervised learning of motion skeleton and latent dynamics from volumetric video. In *Proceedings of the AAAI Conference on Artificial Intelligence*, volume 36, pages 86–94, 2022. 8
- [2] Tom Brown, Benjamin Mann, Nick Ryder, Melanie Subbiah, Jared D. Kaplan, Prafulla Dhariwal, Arvind Neelakantan, Pranav Shyam, Girish Sastry, Amanda Askell, et al. Language models are few-shot learners. *Advances in Neural Information Processing Systems*, 33:1877–1901, 2020. 1
- [3] Holger Caesar, Varun Bankiti, Alex H. Lang, Sourabh Vora, Venice Erin Liong, Qiang Xu, Anush Krishnan, Yu Pan, Giancarlo Baldan, and Oscar Beijbom. nuscenes: A multi-modal dataset for autonomous driving. In *Proceedings of the IEEE/CVF Conference on Computer Vision and Pattern Recognition (CVPR)*, June 2020. 3
- [4] Mathilde Caron, Hugo Touvron, Ishan Misra, Hervé Jégou, Julien Mairal, Piotr Bojanowski, and Armand Joulin. Emerging properties in self-supervised vision transformers. In *Proceedings of the IEEE/CVF International Conference on Computer Vision (ICCV)*, 2021. 1
- [5] Yudi Dai, Yitai Lin, Xiping Lin, Chenglu Wen, Lan Xu, Hongwei Yi, Siqi Shen, Yuexin Ma, and Cheng Wang. Sloper4d: A scene-aware dataset for global 4d human pose estimation in urban environments. In *Proceedings of the IEEE/CVF Conference on Computer Vision and Pattern Recognition (CVPR)*, pages 682–692, June 2023. 3, 6, 7
- [6] Jacob Devlin, Ming-Wei Chang, Kenton Lee, and Kristina Toutanova. Bert: Pre-training of deep bidirectional transformers for language understanding. *arXiv preprint arXiv:1810.04805*, 2018. 1
- [7] Bohao Fan, Siqi Wang, Wenzhao Zheng, Jianjiang Feng, and Jie Zhou. Human-m3: A multi-view multi-modal dataset for 3d human pose estimation in outdoor scenes. *arXiv preprint arXiv:2308.00628*, 2023. 3
- [8] Haoqiang Fan, Hao Su, and Leonidas J Guibas. A point set generation network for 3d object reconstruction from a single image. In *Proceedings of the IEEE Conference on Computer Vision and Pattern Recognition (CVPR)*, pages 605–613, 2017. 5
- [9] Zigang Geng, Ke Sun, Bin Xiao, Zhaoxiang Zhang, and Jingdong Wang. Bottom-up human pose estimation via disentangled keypoint regression. In *Proceedings of the IEEE/CVF Conference on Computer Vision and Pattern Recognition (CVPR)*, pages 14676–14686, 2021. 1
- [10] Thibault Groueix, Matthew Fisher, Vladimir G. Kim, Bryan C. Russell, and Mathieu Aubry. 3d-coded: 3d correspondences by deep deformation. In *Proceedings of the European Conference on Computer Vision (ECCV)*, September 2018. 3
- [11] Chuan Guo, Yuxuan Mu, Muhammad Gohar Javed, Sen Wang, and Li Cheng. Momask: Generative masked modeling of 3d human motions. 2023. 2
- [12] Thorsten Hempel, Ahmed A. Abdelrahman, and Ayoub Al-Hamadi. 6d rotation representation for unconstrained head pose estimation. In *2022 IEEE International Conference on Image Processing (ICIP)*, pages 2496–2500, 2022. 3
- [13] Junjie Huang, Zheng Zhu, Feng Guo, and Guan Huang. The devil is in the details: Delving into unbiased data processing for human pose estimation. In *Proceedings of the IEEE/CVF Conference on Computer Vision and Pattern Recognition (CVPR)*, pages 5700–5709, 2020. 1
- [14] Yinghao Huang, Manuel Kaufmann, Emre Aksan, Michael J. Black, Otmar Hilliges, and Gerard Pons-Moll. Deep inertial poser: Learning to reconstruct human pose from sparse inertial measurements in real time. *ACM Transactions on Graphics (Proc. SIGGRAPH Asia)*, 37:185:1–185:15, Nov. 2018. First two authors contributed equally. 3, 5, 6, 7
- [15] Hojun Jang, Minkwan Kim, Jinseok Bae, and Young Min Kim. Dynamic mesh recovery from partial point cloud sequence. In *Proceedings of the IEEE/CVF International Conference on Computer Vision (ICCV)*, pages 15074–15084, October 2023. 2, 3, 5, 6
- [16] Yifeng Jiang, Yuting Ye, Deepak Gopinath, Jungdam Won, Alexander W. Winkler, and C. Karen Liu. Transformer inertial poser: Real-time human motion reconstruction from sparse imus with simultaneous terrain generation. In *SIGGRAPH Asia 2022 Conference Papers*, SA ’22 Conference Papers, 2022. 3
- [17] Hanbyul Joo, Hao Liu, Lei Tan, Lin Gui, Bart Nabbe, Iain Matthews, Takeo Kanade, Shohei Nobuhara, and Yaser Sheikh. Panoptic studio: A massively multiview system for social motion capture. In *The IEEE International Conference on Computer Vision (ICCV)*, 2015. 5, 6, 8
- [18] Diederik P Kingma and Max Welling. Auto-encoding variational bayes. *arXiv preprint arXiv:1312.6114*, 2013. 3
- [19] Alexander Kirillov, Eric Mintun, Nikhila Ravi, Hanzi Mao, Chloe Rolland, Laura Gustafson, Tete Xiao, Spencer Whitehead, Alexander C. Berg, Wan-Yen Lo, et al. Segment anything. In *Proceedings of the IEEE/CVF International Conference on Computer Vision (ICCV)*, pages 4015–4026, 2023. 1
- [20] Jialian Li, Jingyi Zhang, Zhiyong Wang, Siqi Shen, Chenglu Wen, Yuexin Ma, Lan Xu, Jingyi Yu, and Cheng Wang. Lidarcap: Long-range marker-less 3d human motion capture with lidar point clouds. In *Proceedings of the IEEE/CVF Conference on Computer Vision and Pattern Recognition*, pages 20502–20512, 2022. 3
- [21] Hung Yu Ling, Fabio Zinno, George Cheng, and Michiel van de Panne. Character controllers using motion vaes. *ACM Trans. Graph.*, 39(4), 2020. 2
- [22] Guanze Liu, Yu Rong, and Lu Sheng. Votehmr: Occlusion-aware voting network for robust 3d human mesh recovery from partial point clouds. In *Proceedings of the 29th ACM International Conference on Multimedia*, pages 955–964, 2021. 3, 5, 6
- [23] Matthew Loper, Naureen Mahmood, Javier Romero, Gerard Pons-Moll, and Michael J. Black. SMPL: A skinned multi-person linear model. *ACM Trans. Graphics (Proc. SIGGRAPH Asia)*, 34(6):248:1–248:16, Oct. 2015. 1, 3
- [24] Thomas Lucas\*, Fabien Baradel\*, Philippe Weinzaepfel, and Grégory Rogez. Posegpt: Quantization-based 3d human mo-

- tion generation and forecasting. In *European Conference on Computer Vision (ECCV)*, 2022. [2](#)
- [25] Zhengxiong Luo, Zhicheng Wang, Yan Huang, Liang Wang, Tieniu Tan, and Erjin Zhou. Rethinking the heatmap regression for bottom-up human pose estimation. In *Proceedings of the IEEE/CVF Conference on Computer Vision and Pattern Recognition (CVPR)*, pages 13264–13273, 2021. [1](#)
- [26] Naureen Mahmood, Nima Ghorbani, Nikolaus F. Troje, Gerard Pons-Moll, and Michael J. Black. AMASS: Archive of motion capture as surface shapes. In *Proceedings of the IEEE/CVF International Conference on Computer Vision (ICCV)*, pages 5442–5451, Oct. 2019. [1](#), [2](#), [5](#), [6](#)
- [27] Ferda Ofli, Rizwan Ahmed Chaudhry, Gregorij Kurillo, René Vidal, and Ruzena Bajcsy. Berkeley mhad: A comprehensive multimodal human action database. *2013 IEEE Workshop on Applications of Computer Vision (WACV)*, pages 53–60, 2013. [5](#)
- [28] Long Ouyang, Jeffrey Wu, Xu Jiang, Diogo Almeida, Carroll Wainwright, Pamela Mishkin, Chong Zhang, Sandhini Agarwal, Katarina Slama, Alex Ray, et al. Training language models to follow instructions with human feedback. *Advances in Neural Information Processing Systems*, 35:27730–27744, 2022. [1](#)
- [29] Mathis Petrovich, Michael J. Black, and Gül Varol. Action-conditioned 3d human motion synthesis with transformer vae. In *Proceedings of the IEEE/CVF International Conference on Computer Vision (ICCV)*, pages 10985–10995, October 2021. [2](#)
- [30] Charles R. Qi, Hao Su, Kaichun Mo, and Leonidas J. Guibas. Pointnet: Deep learning on point sets for 3d classification and segmentation. In *Proceedings of the IEEE Conference on Computer Vision and Pattern Recognition (CVPR)*, pages 652–660, 2017. [4](#)
- [31] Alec Radford, Jong Wook Kim, Chris Hallacy, Aditya Ramesh, Gabriel Goh, Sandhini Agarwal, Girish Sastry, Amanda Askell, Pamela Mishkin, Jack Clark, et al. Learning transferable visual models from natural language supervision. In *International Conference on Machine Learning*, pages 8748–8763. PMLR, 2021. [1](#)
- [32] Davis Rempe, Tolga Birdal, Aaron Hertzmann, Jimei Yang, Srinath Sridhar, and Leonidas J. Guibas. Humor: 3d human motion model for robust pose estimation. In *Proceedings of the IEEE/CVF International Conference on Computer Vision (ICCV)*, pages 11488–11499, October 2021. [2](#), [3](#)
- [33] Ke Sun, Bin Xiao, Dong Liu, and Jingdong Wang. Deep high-resolution representation learning for human pose estimation. In *Proceedings of the IEEE/CVF Conference on Computer Vision and Pattern Recognition (CVPR)*, pages 5693–5703, 2019. [1](#)
- [34] Pei Sun, Henrik Kretschmar, Xerxes Dotiwalla, Aurelien Chouard, Vijaysai Patnaik, Paul Tsui, James Guo, Yin Zhou, Yuning Chai, Benjamin Caine, Vijay Vasudevan, Wei Han, Jiquan Ngiam, Hang Zhao, Aleksei Timofeev, Scott Ettinger, Maxim Krivokon, Amy Gao, Aditya Joshi, Yu Zhang, Jonathon Shlens, Zhifeng Chen, and Dragomir Anguelov. Scalability in perception for autonomous driving: Waymo open dataset. In *Proceedings of the IEEE/CVF Conference on Computer Vision and Pattern Recognition (CVPR)*, June 2020. [3](#)
- [35] Matt Trumble, Andrew Gilbert, Charles Malleson, Adrian Hilton, and John Collomosse. Total capture: 3d human pose estimation fusing video and inertial sensors. In *2017 British Machine Vision Conference (BMVC)*, 2017. [6](#), [7](#)
- [36] Aaron Van Den Oord, Oriol Vinyals, et al. Neural discrete representation learning. *Advances in Neural Information Processing Systems*, 30, 2017. [2](#)
- [37] Gül Varol, Javier Romero, Xavier Martin, Naureen Mahmood, Michael J. Black, Ivan Laptev, and Cordelia Schmid. Learning from synthetic humans. In *IEEE Conference on Computer Vision and Pattern Recognition (CVPR)*, 2017. [5](#)
- [38] Ashish Vaswani, Noam Shazeer, Niki Parmar, Jakob Uszkoreit, Llion Jones, Aidan N Gomez, Łukasz Kaiser, and Illia Polosukhin. Attention is all you need. In I. Guyon, U. Von Luxburg, S. Bengio, H. Wallach, R. Fergus, S. Vishwanathan, and R. Garnett, editors, *Advances in Neural Information Processing Systems*, volume 30. Curran Associates, Inc., 2017. [3](#)
- [39] Timo Von Marcard, Bodo Rosenhahn, Michael J. Black, and Gerard Pons-Moll. Sparse inertial poser: Automatic 3d human pose estimation from sparse imus. In *Computer Graphics Forum*, volume 36, pages 349–360. Wiley Online Library, 2017. [3](#)
- [40] Xinyu Yi, Yuxiao Zhou, Marc Habermann, Soshi Shimada, Vladislav Golyanik, Christian Theobalt, and Feng Xu. Physical inertial poser (pip): Physics-aware real-time human motion tracking from sparse inertial sensors. In *Proceedings of the IEEE/CVF Conference on Computer Vision and Pattern Recognition (CVPR)*, pages 13167–13178, June 2022. [3](#), [6](#), [8](#)
- [41] Xinyu Yi, Yuxiao Zhou, and Feng Xu. Transpose: Real-time 3d human translation and pose estimation with six inertial sensors. *ACM Transactions on Graphics*, 40(4), 08 2021. [3](#), [6](#)
- [42] Feng Zhang, Xiatian Zhu, Hanbin Dai, Mao Ye, and Ce Zhu. Distribution-aware coordinate representation for human pose estimation. In *Proceedings of the IEEE/CVF Conference on Computer Vision and Pattern Recognition (CVPR)*, pages 7093–7102, 2020. [1](#)
- [43] Zhengyou Zhang. Microsoft kinect sensor and its effect. *IEEE multimedia*, 19(2):4–10, 2012. [5](#)
- [44] Qian-Yi Zhou, Jaesik Park, and Vladlen Koltun. Open3D: A modern library for 3D data processing. *arXiv:1801.09847*, 2018. [5](#)
- [45] Xinxin Zuo, Sen Wang, Qiang Sun, Minglun Gong, and Li Cheng. Self-supervised 3d human mesh recovery from noisy point clouds. *arXiv preprint arXiv:2107.07539*, 2021. [3](#), [5](#), [6](#)